Processing and Wear Testing of Novel High-Hardness Wear-Resistant Steel

O. Haiko[1*], I. Miettunen[1], D. Porter[1], N. Ojala[2], V. Ratia[2], V. Heino[2], A. Kemppainen[3]

[1]*University of Oulu, Faculty of Technology, Materials Engineering and Production Technology, POB 4200, 90014 Oulu, Finland.*
[2]*Tampere University of Technology, Department of Materials Science, Tampere Wear Center, POB 589, 33101 Tampere, Finland.*
[3]*SSAB Europe, POB 93, 92101 Raahe, Finland*

Abstract

Novel high-hardness medium carbon martensitic laboratory steel has been produced and tested for wear resistance. Different finish rolling temperatures (FRT) and quenching finish temperatures (QFT) were utilized. Composition was selected based on earlier experiments and carbon content was set to 0.35 % to obtain surface hardness of approximately 600 HB. FRT was varied to investigate the effect of prior austenite deformation on the mechanical properties. Direct quenching was implemented in the laboratory rolling trials. Plates were either quenched to room temperature or quenching was finished at 250 °C. The interrupted quenching was tested in order to improve the toughness of the steel via autotempering and possible austenite retention without drastic loss of hardness. The steel samples were tested for hardness and impact toughness. Material characterization included SEM and optical microscopy for microstructural inspection. Direct quenched steel samples exceeded the desired 600 HB surface hardness, but interrupted quenching to 250 °C resulted in lower hardness values. In contrast, the impact toughness was improved with latter quenching method. Impact-abrasion wear testing was conducted for the experimental steels to understand the effect of rolling and quenching parameters on wear resistance. Impeller-tumbler tests were carried out at Tampere Wear Center using natural granite as the abrasive. The results indicate that surface hardness is the main controlling factor of wear, and samples with the highest surface hardness showed the lowest mass loss.

Keywords: wear, steel, impact abrasion, hardness

*Corresponding author: Oskari Haiko (oskari.haiko@oulu.fi).

1. INTRODUCTION

Abrasive and impact wear are often present in the severe conditions of mining, mineral processing, earth-moving and agricultural industries. Rocks, sand and gravel cause heavy wear by sliding, impacting or grooving on the surface subjected to wear. High-hardness steels are commonly used as wear-resistant materials in many applications. The wear resistance is often considered to be related to the surface hardness of the steel. Commercial wear-resistant steels are available in different hardness grades ranging from 400 Brinells up to 600 HB. The higher hardness is usually obtained by increasing the carbon content of the steel. However, the higher carbon content normally leads to limited usability. Toughness, bendability and weldability properties are deteriorated. Hence, other methods are utilized to increase the hardness of steel without drastic loss of other important properties.

Direct quenching (DQ) has been utilized for producing similar steels with leaner alloying. Thermomechanically controlled processing (TMCP) has been introduced for refining the grain size. Both of the processing methods are nowadays used for production of ultra-high strength steels [1-3]. Finer grain size is obtained by controlled rolling in the non-recrystallization regime (NRX). Strain is applied to austenite, which leads to increased dislocation density and elongated grain structure. Finish rolling temperature (FRT) should be low enough for reduction to take place in the NRX regime. Direct quenching is applied after the finishing pass. This approach gives increased strength and toughness without a major loss of ductility [2].

The balance between impact toughness and hardness is often a trade-off in high-hardness steels. Super high-hardness steels may exhibit very low impact toughness values below room temperature. Adopting TMCP and DQ improves the impact toughness, but transition temperatures might still remain relatively high. In earlier research this problem was tried to solve by introducing small amounts of ferrite into the martensitic matrix

[4]. The amount of ferrite was realised to be difficult to control and this approach was dismissed. Hence, a new cooling method was applied to improve the impact toughness properties. Water quenching was interrupted at 250 °C and the rolled plates were then cooled in air. Quenching finish temperature (QFT) was set between the martensite start (M_s) and finish (M_f) temperatures. The aim was to induce autotempering effects and possible austenite retention to improve the impact toughness [5-7].

Impeller-tumbler wear testing device was selected as an appropriate method to test the wear performance. The apparatus is an impact-abrasion wear tester that allows the use of natural granite as the abrasive. The test setup simulates the harsh impact-abrasive tribosystem found in mining and mineral processing environment. Materials are subjected heavy surface deformation during testing. Mass loss of the specimens is measured during and after the wear testing. Material examination included microstructural characterization in both initial and worn state. Mechanical testing was conducted by measuring surface hardness and impact toughness properties. The purpose of the work was to investigate the effect of different rolling and quenching parameters on the wear resistance.

2. EXPERIMENTAL

2.1 Materials and laboratory rolling experiments

The chemical composition of the laboratory steel is presented in Table 1. The initial plan was to produce fully martensitic microstructure via direct quenching and martensite-retained austenite mixture with interrupted quenching. The carbon content of 0.35 % was estimated to be sufficient to reach 600 HB hardness level with direct the quenched variants [8]. The composition was designed to have balanced properties for strength, hardness and impact toughness for improved wear resistance. The emphasis was also to have better usability and manufacturability.

Table 1: *Chemical composition of the laboratory steel (wt-%, balance Fe).*

C	Si	Mn	Al	V	Ti	Cr	Ni	Mo
0.349	0.250	0.510	0.033	0.0014	0.0028	0.770	2.000	0.150

The slab annealing temperature was 1200 °C for 2 hours to produce even grain size. The slab size was 140 x 80 x 60 mm. Slabs were rolled from 60 mm to final thickness of 9 mm with total reduction of 85 %. The hot rolling schedule included three different finish rolling temperatures (FRT) 920, 850 and 780 °C for varying the rolling below the non-recrystallization temperature (T_{nr}). The T_{nr} was estimated to be around 950 °C by using equation by Barbosa et al. [9]. The rolled plates were direct quenched immediately after final rolling pass. Quenching was either continued to room temperature or interrupted at 250 °C. Subsequent air cooling was applied after reaching the quenching finish temperature (QFT). The calculated M_s temperature was 325-330 °C (Andrews product and linear) [8]. The quenching finish temperature (250 °C) was below the M_s temperature in order to produce martensitic microstructure with small amount of retained austenite.

2.2 Microstructural characterization and mechanical testing

Optical, laser and electron microscopes were utilized for microstructural characterization. Keyence VK-X200 laser microscope was used for inspection of the prior austenite grain size, microstructure and wear surfaces. More detailed microstructural inspection was carried out with Zeiss Sigma field emission scanning electron microscope (FESEM). The samples were polished and etched with either picric acid (prior austenite grain size) or nital 4 % (microstructure). The prior austenite grain size was measured with linear intercept method from planar sections [10]. X-ray diffraction (XRD) measurements were conducted with Siemens D5000 device to reveal the retained austenite.

Mechanical testing included only hardness and impact toughness measurements due to the small amount of material produced. Surface hardness was measured with Struers Duramin A-300 hardness tester. The load was 10 kg and Vickers HV hardness scale was used. The hardness of 600 Brinells corresponds to 630-640 in Vickers HV10 scale. Surface hardness was measured from the prepared wear test samples prior to wear testing. Charpy-V testing was conducted for measuring the impact toughness and the temperature range for testing was from -80 to 120 °C. Two samples in longitudinal to rolling direction were tested for each

temperature per steel variant. The Charpy-V sample size was sub-size, 10 x 7.5 x 55 mm. Impact testing was not continued to lower temperatures if impact energy did not reach 20 joules.

2.2 Wear testing

Wear testing was conducted at Tampere Wear Center facilities in Tampere University of Technology, Tampere, Finland. TWC accompanies a wide variety of standardized and modified wear test equipment. The laboratory steels were tested with impeller-tumbler that simulates heavy impact-abrasive wear [11]. The apparatus includes the impeller part with sample holder and the tumbler, in which the gravel is placed. Both parts rotate to the same direction. Samples are attached to the impeller sample holder that can hold three samples at a time. One of the samples is normally a reference sample. Impeller rotates inside the tumbler and samples hit the abrasives with high velocity. Tumbler keeps the gravel moving and impacting the samples. Here, the impeller rotation speed was set to 700 rpm and the tumbler 30 rpm, respectively. Tumbler diameter is 350 mm.

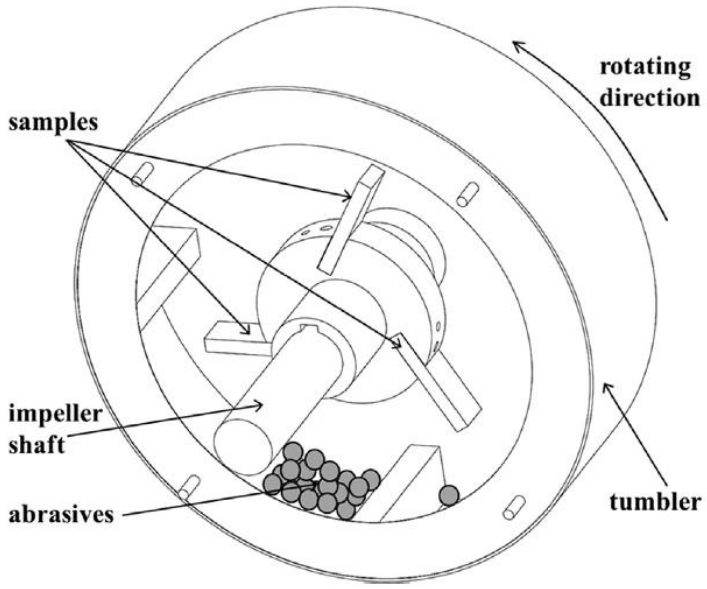

Figure 1: *Impeller-tumbler wear testing device illustrated [11].*

Samples were at 60° angle to the sample holder perimeter. The abrasives are loose inside the tumbler resulting in that the abrasive incident angle is not necessarily same as the sample angle. Natural granite was used as abrasive material and size distribution was 10-12.5 mm, each batch having the mass of 900 g. Gravel was renewed every 15 minutes and mass loss of the samples was measured also at 15 min intervals. The duration of the actual test was 60 min. Before the actual test, the testing procedure included a 15 min interval as running-in phase to reach steady-state wear. Sample holder has three slots of which one slot was reserved for the reference material. The two actual test material samples were rotated between slots 1 and 2 at every 15 minutes, but reference material was kept in slot 3 throughout the test for comparability. The sample size was 71 x 24 x 7.8 mm and two samples were tested per variant. An illustration of the device is presented in Figure 1.

3. RESULTS

3.1 Microstructures

FESEM images of the microstructures of tested specimen are given in Figure 2. Direct quenched steels are referred as DQ variants and the steels with interrupted quenching are referred as QFT or -250 variants. The lath-like martensitic structure can be distinguished, and both packets and blocks are also visible. The major difference between the DQ and QFT samples is the amount of rod-shaped carbides present in the microstructure. This is clearly seen in the 780 and 850 QFT variants. White, larger carbon-rich areas can be

found in the QFT samples which indicates that more tempering effects have occurred. The interrupted quenching has enabled longer time for autotempering to take place. However, any larger islands of retained austenite cannot be observed from the FESEM images.

Table 2: *Prior austenite grain size: ND is normal and RD rolling direction, AR stands for aspect ratio and L is the mean linear intercept value for prior austenite grain size.*

FRT	L_{ND} (µm)	L_{RD} (µm)	AR	L (µm)
780	7.83±0.33	32.65±1.48	4.17	15.99
850	12.63±0.52	29.28±1.34	2.32	19.23
920	13.09±0.57	18.43±0.79	1.41	15.53

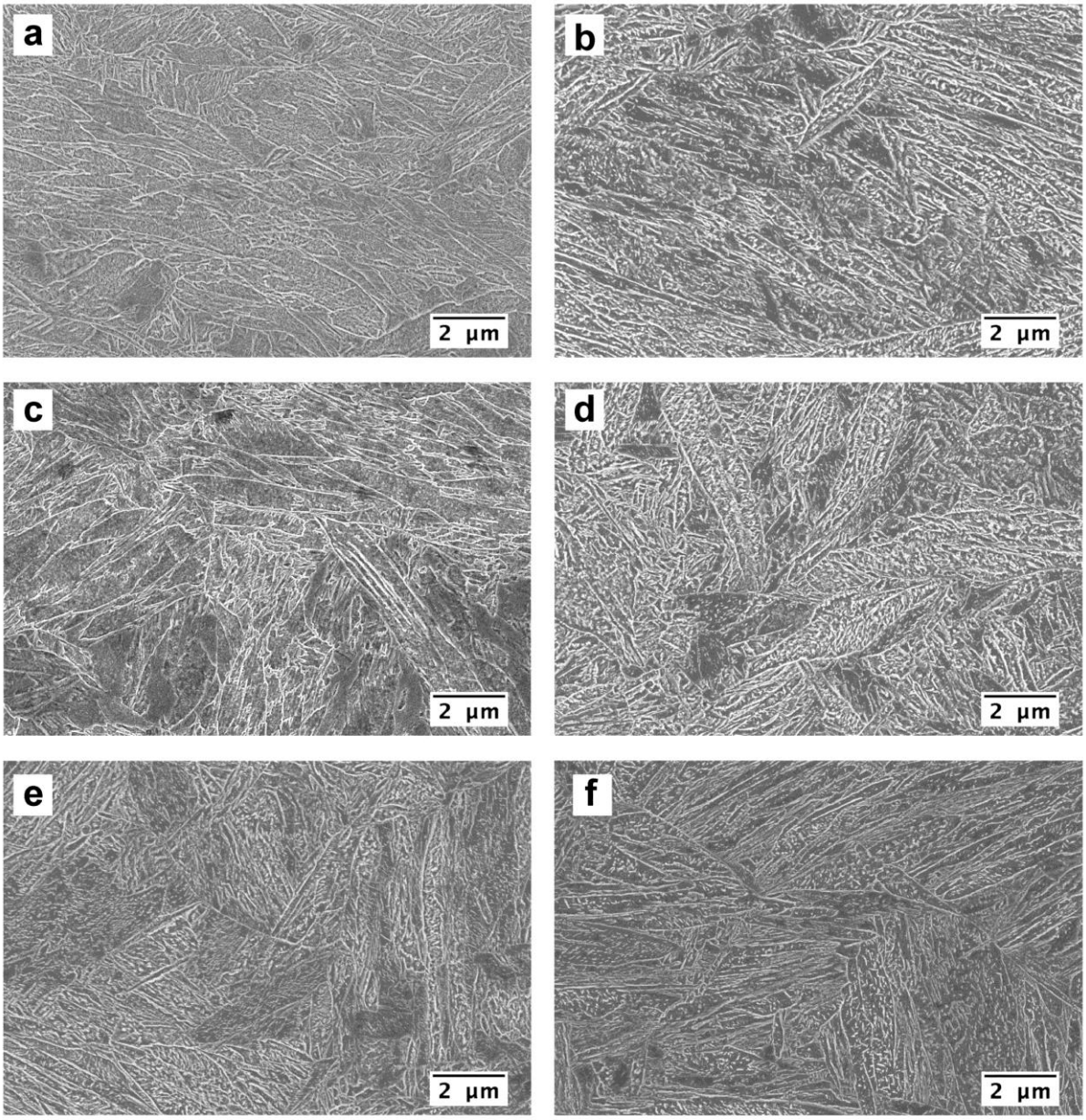

Figure 2: *FESEM images of the tested steels: (a) 780-DQ, (b) 780-250, (c) 850-DQ, (d) 850-250, (e) 920-DQ and (f) 920-250.*

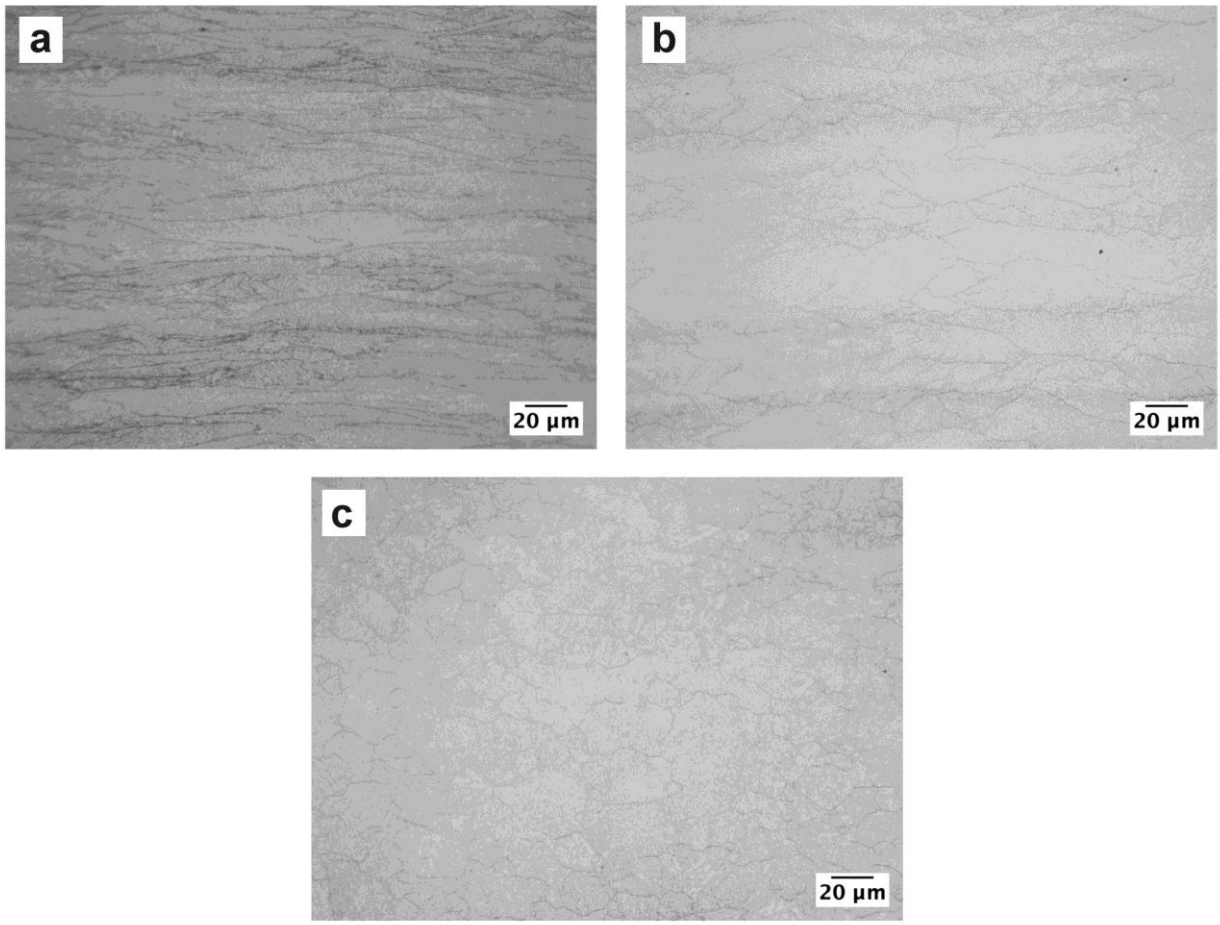

Figure 3: *Optical microscope images of the samples etched to reveal prior austenite grain size: (a) 780-DQ, (b) 850-DQ and (c) 920-DQ.*

More profound difference is found in the prior austenite grain size. Figure 3 shows the effect of decreasing finish rolling temperature. Grain structure is clearly more pancaked in the lower FRT samples. Controlled rolling in the non-recrystallization regime has produced more distorted grain structure. Austenite grains have been flattened and grains appear elongated. The prior austenite grain size was determined by linear intercept method by Higginson et al. [10] from normal and rolling direction and the results are given in Table 2. The table also includes 95 % confidence limits, aspect ratio and the overall mean linear intercept (L) value for the grain size. The aspect ratio increases drastically with decreasing finish rolling temperature, while the overall grain size stays nearly the same for 780 and 920 FRT variants. Thus, the grain structure might be very distorted or nearly equiaxed with the same overall mean linear intercept. Nevertheless, the more distorted and elongated grain structure may exhibit higher grain boundary area per unit volume (S_v) and increased dislocation density.

3.2 Mechanical properties

Surface hardness and impact toughness properties for the tested steels are presented in Table 3. Realised finish rolling and quenching finish temperatures are shown. Average deviation for the hardness results was 3.16 %. The highest surface hardness was measured from the direct quenched samples, nearly 700 HV. There were no great differences in the hardness values of the DQ samples. Lowering the finish rolling temperature did alter the grain structure, but hardness was not affected. In contrast, the interrupted quenching clearly decreased the surface hardness. Almost 200 HV decrease was measured between the 920 DQ and QFT variants.

Table 3: *Realised rolling parameters, surface hardness values, estimated T20J temperatures and retained austenite content (RA).*

Material	FRT (°C)	QFT (°C)	HV10	T20J (°C)	RA (%)
780-DQ	750	20	695	70	2.3
850-DQ	850	20	680	100	1.7
920-DQ	890	20	687	100	1.4
780-250	775	235	648	-55	4.2
850-250	840	235	611	-60	2.5
920-250	900	260	505	-60	3.1

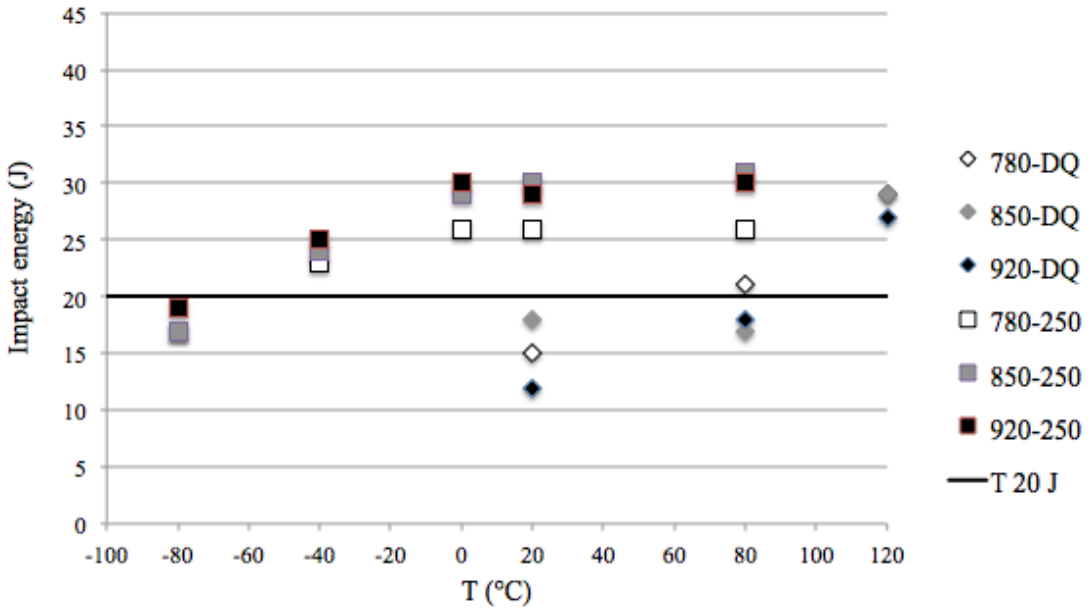

Figure 4: *Charpy-V impact test results.*

A threshold limit of 20 joules was selected for the impact toughness measurements. The initial goal was to achieve both 600 HB hardness and 20 joule impact energy at -40 °C**.** The elongated grain structure does seem to improve the T20J temperature for the 780-DQ sample, but the T20J estimations should be treated with care due to the small amount of tested specimens. The direct quenched samples have very high transition temperatures compared to the interrupted quenching variants. The Charpy-V impact energies are very close to each other with the QFT samples. Impact energies are given in Figure 4.

3.3 Impeller-tumbler wear tests

The impeller-tumbler wear test results with standard deviation are given in Figure 5. The highest mass loss (0.197 g) was measured for test variant 920-250 which also exhibited the lowest surface hardness (505 HV). The other two QFT variants had quite interestingly nearly the same mass loss despite 40 HV hardness difference. In contrast, all the DQ variants showed very similar hardness values compared to each other, and almost 700 HV limit was reached. The wear test results are also in line, and no there are no great differences regarding mass loss with DQ samples. Generally, the increasing hardness did improve the wear resistance. Here, the material 920-250 had 38 % higher mass loss when compared to best performing material, 780-DQ. In turn, the 780-DQ showed 38 % greater surface hardness than 920-250. The correlation between surface hardness and mass loss seems to apply fairly well.

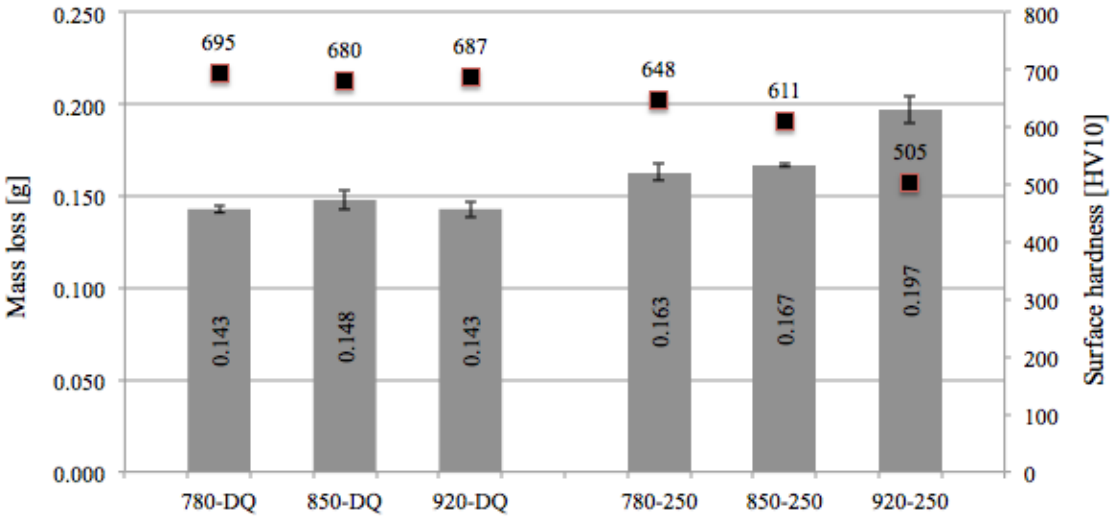

Figure 5: *Impeller-tumbler wear test results with standard deviation and surface hardness values.*

The wear surfaces were examined with both laser and scanning electron microscopes. Figure 6 shows the impeller tumbler samples in unworn and worn condition. The impeller-tumbler wear testing device causes heavy edge-concentrated wear as the samples are rotating inside the tumbler. Figure 7 shows the laser microscope images of the edges of worn samples. The worn samples were cut in half along the longitudinal axis for cross-sectional wear surface inspection. The direct quenched variants are on the left and the interrupted quenching variants on the right. Comparing the least (a) and the most (f) worn samples does not clearly reveal any substantial differences. However, a closer examination unveils that sample 920-250 (f) has slightly more dented or rougher edge. It should be noted that the mass loss during test period is less than 200 milligrams. Surface profile measurements were also done for the worn samples and the results are presented in Table 4. The surface roughness values are fairly consistent with the measured mass losses.

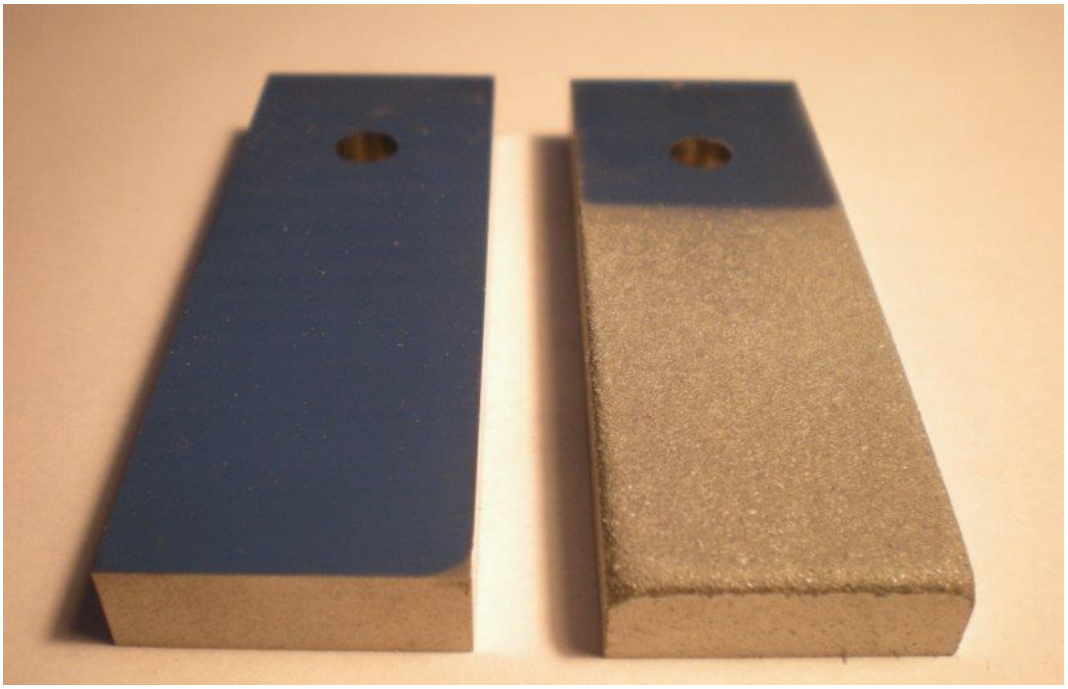

Figure 6: *Unworn (left) and worn (right) impeller-tumbler samples.*

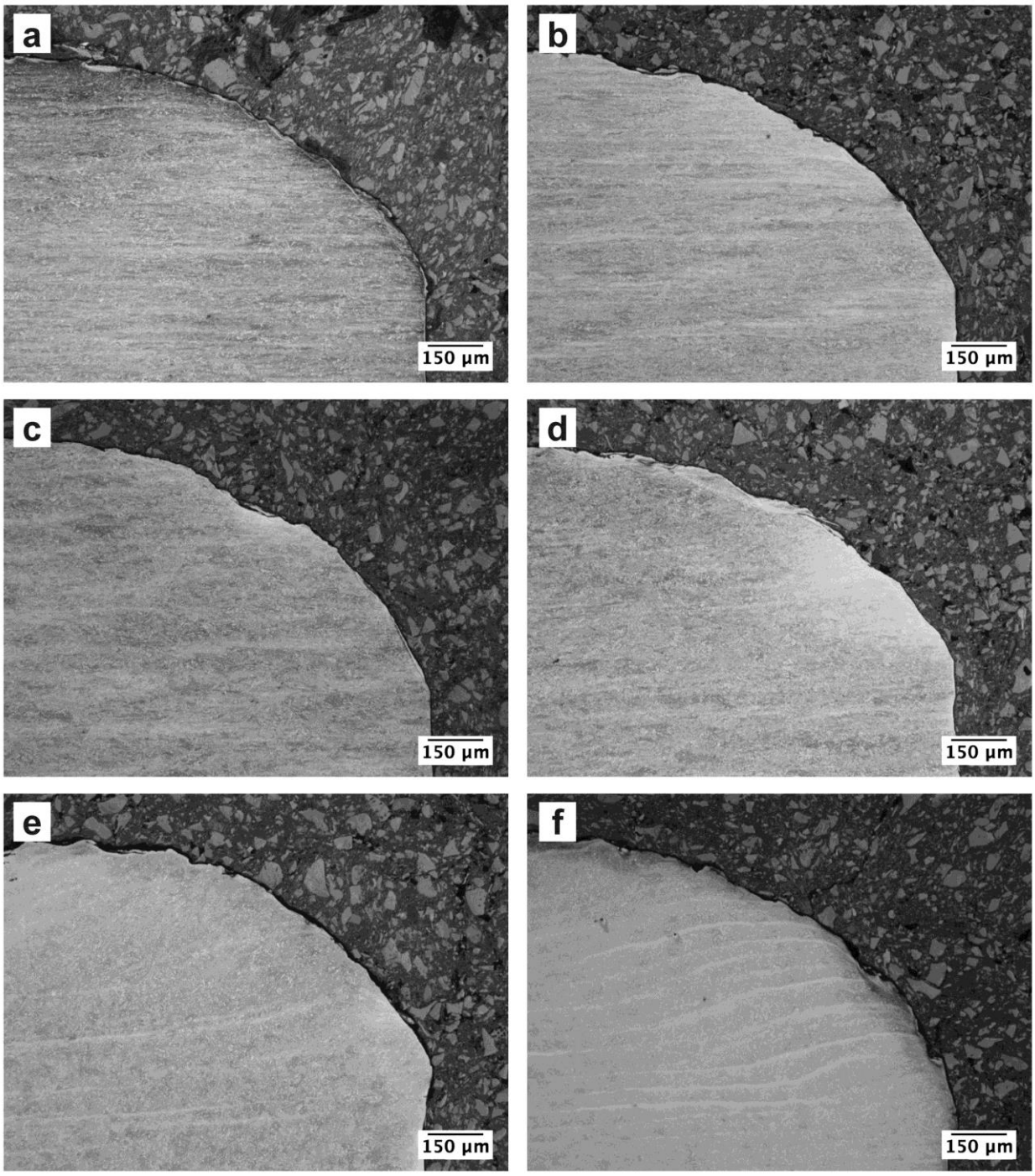

Figure 7: *Impeller-tumbler test specimen: (a) 780-DQ, (b) 780-250, (c) 850-DQ, (d) 850-250, (e) 920-DQ and (f) 920-250.*

Table 4: *Measured surface roughness values for worn samples.*

Material	Ra (µm)	Rq (µm)	Rz (µm)
780-DQ	5	6	79
850-DQ	5	6	76
920-DQ	5	6	74
780-250	6	8	89
850-250	6	8	99
920-250	7	10	111

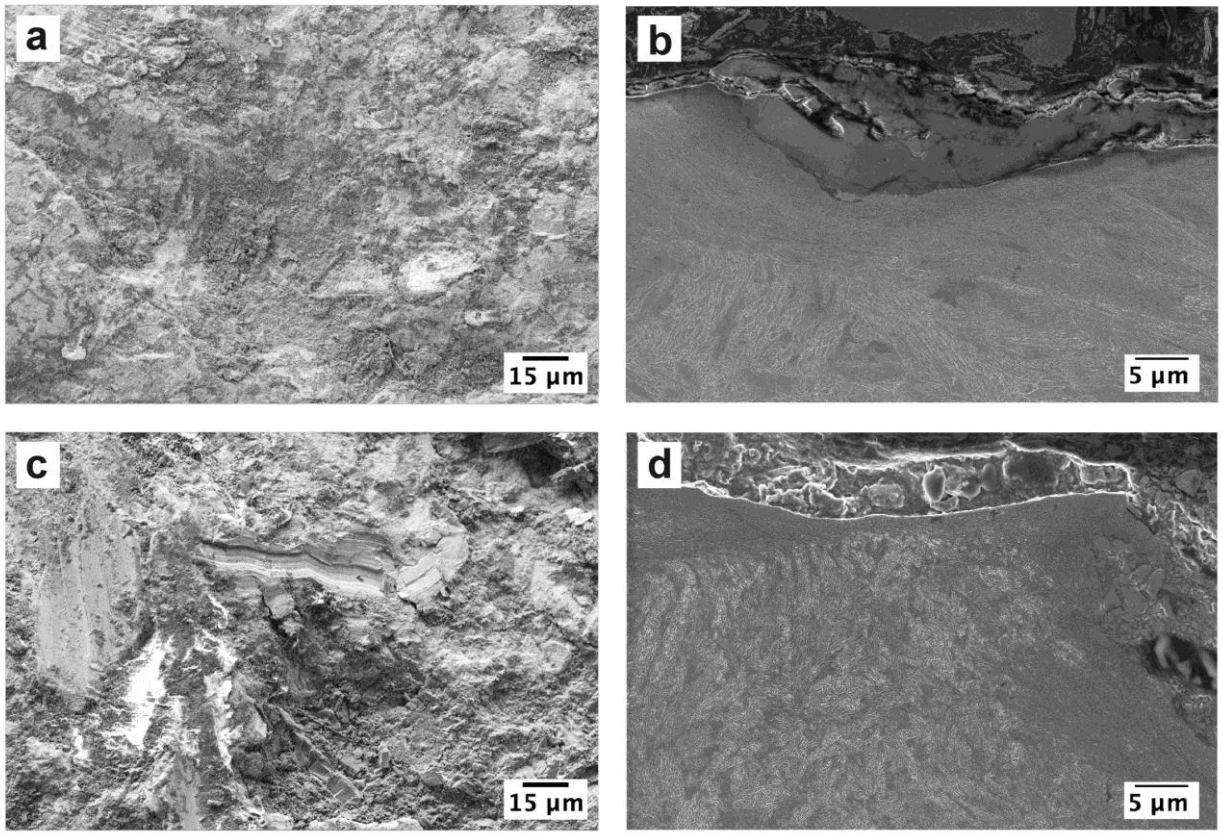

Figure 8: *FESEM images of worn surfaces and cross-section of the same specimens: (a) 780-DQ surface, (b) 780-DQ cross –section, (c) 920-250 surface and (d) 920-250 cross-section.*

The worn surfaces and cross-sections of the impeller-tumbler samples are shown in Figure 8**.** The FESEM images reveal embedded granite and heavily deformed microstructure near the surface. The depth of the affected layer is generally less than 40 µm. Most areas only show few microns of deformed structure. The high hardness of the steels has clearly prevented greater penetration of the granite. Scratch marks are visible and wear mode appears to have been mostly abrasive. Cross-sectional images show some larger craters and also some small areas that appear to have been peeled or fractured off the surface.

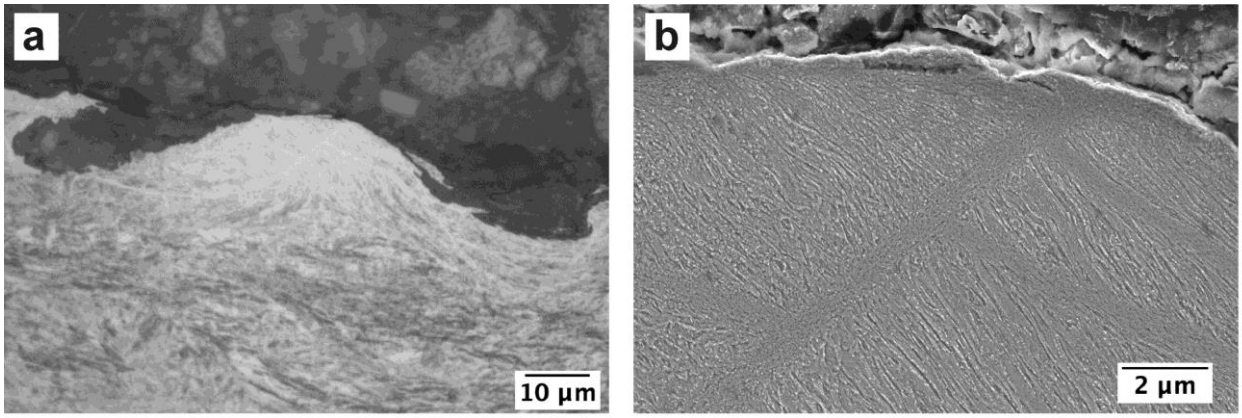

Figure 9: *Optical (a) and electron microscope (b) image of shear bands (sample 850-250).*

Shear bands were discovered in all tested samples. The bands appear white in optical microscope images and darker in FESEM images (Figure 9). A closer look of the bands reveals very fine microstructure, nearly nano-sized grains. These fine structures were found close to the surface. Another interesting feature is the orientation and fibering phenomenon of the martensite laths on the deformed layer near the surface. The laths have clearly bent and orientated, and they also appear elongated. The impact energy has been great enough to cause plastic flow in all samples.

4. DISCUSSION

The present work has shown that hardness is the main controlling factor of wear for the tested martensitic steels. The materials with higher initial surface hardness proved to show better wear performance, and the lowest mass losses during wear testing were measured for the samples with the highest initial hardness. Wear testing was done with impeller-tumbler impact-abrasion wear testing device. Different finish rolling temperatures were applied during hot rolling to examine the effect on grain structure. Direct quenching and interrupted quenching were implemented. The latter was utilized to improve the impact toughness properties of the steels and to understand how impact toughness affects wear performance.

The rolling schedule was varied to alter the prior austenite grain structure. The aim was to produce more distorted, pancaked grains by rolling in the non-recrystallization regime. The finishing passes at 850 and 780 °C produced elongated grains with higher aspect ratio compared to 920 °C FRT. Calculated T_{nr} was 951 °C. The micrographs of the grain structure support this, as rolling near 900 °C already shows slightly deformed austenite grains. The total reduction (R_{tot}) in the NRX regime and subsequent flat, pancaked grain structure has been attributed to improved impact toughness and strength properties [2-3]. This is derived from the increased total surface area per unit volume ($S_{v(tot)}$) by the amount of austenite grain boundaries and deformation bands of austenite [12]. Work by Kaijalainen et al. [2-3; 12] showed that increased strength, impact toughness and fracture properties for low-carbon direct quenched steels can be achieved by increasing reduction in the NRX regime. Decreasing the FRT from 920 to 860 °C improved the impact energy at -40 °C for medium carbon abrasion resistant martensitic steel in the work of Deng et al. [13]. Ouchi [1] also notes that increased cumulative rolling below temperature range of austenite recrystallization is utilized to achieve superior low temperature impact toughness with line pipe steels. Thermo-mechanical processing has been already discussed in the 1970's as a novel method for improving impact toughness without loss of strength [14]. Conversely, Bracke et al. [15] reported increased strength and decreased impact toughness for rolling in the non-recrystallization regime. Prior austenite grain aspect ratio between 2 and 4 resulted in deteriorated impact toughness at -20 and -40 °C. However, aspect ratio greater than 4 increased the impact toughness to the same level with the equiaxed grain structure. In this work, the estimated T20J value did show some improvement with decreasing FRT. Though, the amount of impact tests was fairly low and complete transition curves were not plotted. The absolute values at 20 °C for DQ samples were 12 J for 920-DQ, 18 J for 850-DQ and 15 J for 780-DQ indicating very low toughness in lower temperatures. It is evident in this work that the impact toughness is not drastically changed with the distorted grain structure. This applies for both DQ and QFT samples.

The major improvement with impact toughness was achieved with the interrupted quenching. Stopping the water quenching at 250 °C and subsequent air cooling resulted in higher transitions temperatures. All the QFT variants had impact toughness of 20 joules below -40 °C, as none of the DQ samples reached 20 joules below 50 °C. The initial idea for the stopped quenching was derived from the novel quenching and partitioning processing method. Q&P processing involves quenching below M_s temperature to initiate the martensite transformation and then isothermal hold is applied to stabilize the retained austenite [16-17]. In this work, the isothermal hold was not applied and the plates were cooled in air after interrupted quenching. This was done in order to simulate industrial processing when isothermal hold is not an option. Thomas et al. [5] also discuss non-isothermal partitioning with large coil products. Tan et al. [6] refer to dynamical partitioning when quenching is stopped between M_s and M_f temperatures. The aim in both Q&P and dynamical partitioning is to produce room temperature stable austenite by the partitioning process. This occurs by the diffusion of carbon from martensite to austenite. In dynamical partitioning, the carbon content of the retained austenite is lower since there is less time for diffusion. However, the lower carbon content of the retained austenite might induce easier transformation to martensite [6]. Thus, the more responsive TRIP effects could provide an interesting feature in the dynamically partitioned steels. The stability and morphology of the retained austenite affect the impact toughness properties. The film-like austenite between laths improves the impact toughness, but granular islands might deteriorate the properties. The effect is related to finer effective grain size. The film-like austenite will transform under load to martensite with orientation very different from that of the surrounding packet and it does not share the {100} cleavage planes with it [18]. This effect only lowers the ductile-to-brittle transformation temperature (DBTT) and does not improve impact toughness in ductile mode. There have been also suggestions for optimum fraction of retained austenite for improved impact toughness. Thus, the best balance between strength, ductility and

toughness is should be achieved with fine, film-like austenite between the martensite laths with 7-15 % content of retained austenite [19].

The QFT samples in this work included 2.5-4.2 % retained austenite, but impact toughness was improved drastically. The main reason for the improved impact toughness is the lower yield strength drawn from both increased austenite content and autotempering of martensite. Brittle fracture in ferritic (including martensitic) steels starts to happen when temperature falls enough for stress required for plastic flow to rise above that required for cleavage [20]. This means that brittle-to-ductile transformation temperature depends on both yield strength and fracture toughness. The fracture mode was fully brittle in 20 °C for the tested DQ variants. The QFT variants had mixed ductile-to-brittle fracture. The fracture toughness in ductile mode is also highly dependent on the yield strength, meaning that the impact toughness can always be increased by lowering the strength [21]. The possible effect of increased austenite content on fracture strength is therefore very difficult to measure. Granular islands of retained austenite were not observed from the FESEM images, but very thin films of austenite could not be detected as well. Transmission electron microscope (TEM) is required to observe the martensite laths more carefully.

Decreasing the finish rolling temperature seems to affect the hardness loss caused by interrupted quenching. Surface hardness did not decrease as much with the lower finish rolling temperature for QFT samples. While the impact toughness is almost the same for all QFT samples, there was a significant drop of hardness with increasing FRT. Thus, the 780-250 variant shows very promising balance of hardness and toughness. The material reached higher than 600 HB surface hardness with impact toughness of around 23 joules at -40 °C. However, the realised quenching finish temperature for 920-250 was slightly higher compared to 780-250 and 850-250, which might explain the loss of hardness. Nevertheless, it seems that here the lowest FRT steel preserved the hardness better than the other QFT variants.

The wear performance increases with increasing surface hardness despite drastically deteriorated impact toughness. Figure 10 shows the correlation between hardness and mass loss for the tested impeller-tumbler samples. It has been well known that the wear resistance of steels increases with increasing hardness. Nowadays, this has been shown to apply for the same type of microstructures, but the wear performance varies between different microstructures for a given hardness [22-24]. The studied steels all exhibited martensitic microstructure, even though the amount of retained austenite varied slightly. Thus, the correlation of mass loss and hardness agrees with literature. The impact toughness properties did not seem to affect the wear performance. The toughness at room temperature was sufficient to withstand the impact wear caused by the impeller-tumbler. It should be also noted that Charpy-V impact toughness test with notched sample does not represent wear conditions. Even though toughness is considered important factor for wear resistance, notched impact toughness tests are not the most suitable for determining the wear performance. More important properties regarding toughness are reduced tendency to crack propagation, fracture and material detachment [22]. Still, Charpy-V impact toughness is an important measure for steel usability in structures.

The inspection of the worn surfaces showed that microploughing, microcutting and some microcracking had occurred. Abrasive wear had caused distinct marks on the samples and some granite had been embedded to the surfaces. The energy of the impacting particles has been great enough to cause severely deformed microstructure, but penetration depth is quite low. Also, shear bands were found in both DQ and QFT samples. The white bands consist of very fine martensite, and are referred as transformed bands in steels. The adiabatic shear bands have been associated with brittle fracture [25]. Many of the tested steels showed shear bands evolved underneath the surface. The direction of the band varies as some bands were parallel to the elongated grains, but some were perpendicular. Abrasives impact the surface from multiple directions and hence the shear bands may also form in different directions. The surface roughness measurements also prove that the samples with greater mass loss have rougher surface. The R_z values (the absolute vertical distance between the highest peak and the deepest valley) were higher for more worn samples. The high R_z values indicate that there are deeper scratches or valleys on the sample surface.

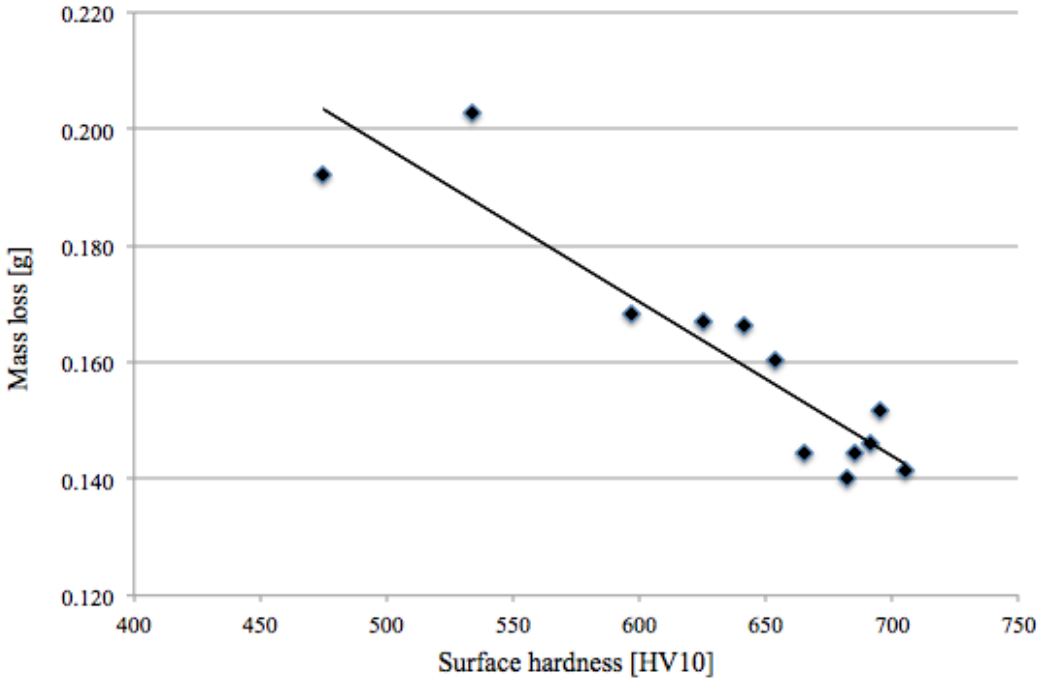

Figure 10: *Mass loss and surface hardness of all tested samples.*

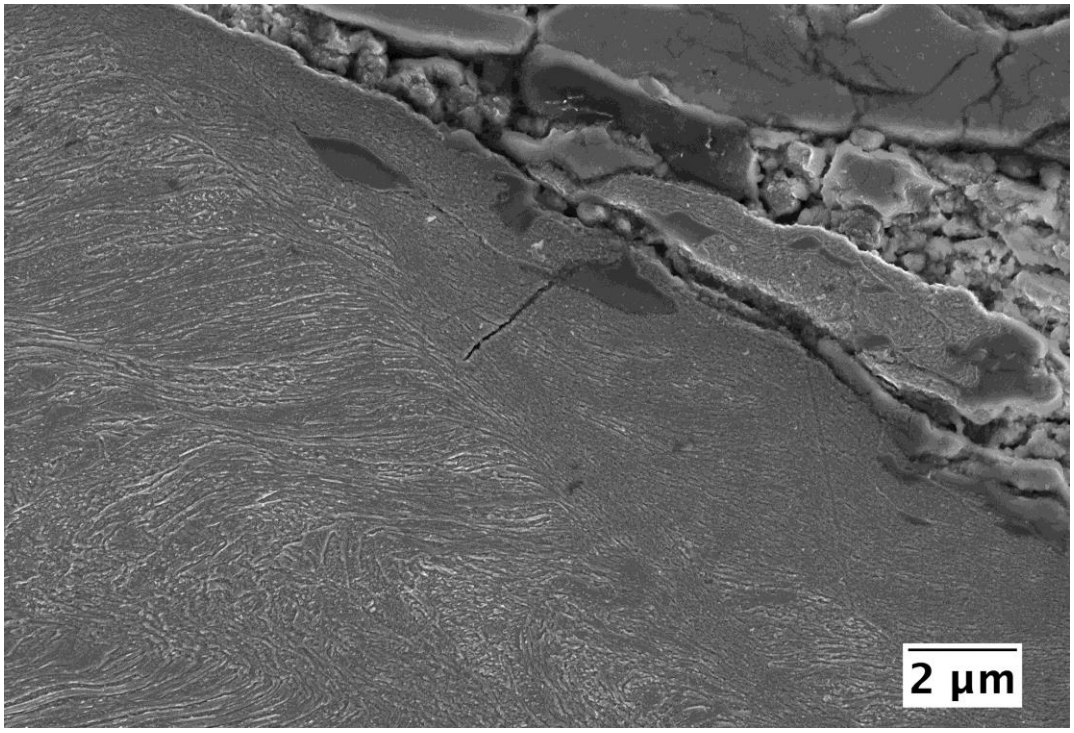

Figure 11: *FESEM image of martensite laths bending and fibering (sample 850-250).*

The strong fibering of martensite laths was discovered near the surface (Figure 11). This has been observed earlier in the impeller-tumbler tests with 400-650 HB hardness grade steels [26], but also in crushing pin-on-disk tests with 400 HB wear-resistant steels [27]. Very fine microstructure could be seen near the surface, similar to the shear band structure, often referred as white layer. This indicates that brittle fracture has happened and some parts of the surface layer might have fractured and peeled off. Comparison between the most worn (920-250) and the best performing sample (780-DQ) shows that there is more coverage by white layer on the surface of the 920-250 and the layer is also thicker. In contrast, the 780-DQ has much smoother surface with less white deformed sections. Sample 920-250 seems to have work hardened more, but this has not prevented the cracking of the surface. It has been suggested that some softer steels show better wear

performance due to good work hardening capability, but the transition from hard tribolayer to bulk should be smooth [27]. Now the hard layer can be cracked by the repeated impacts. Figure 12 shows an embedded granite particle and cracked white layer in sample 920-250. Softer multi-phase microstructures have proven to be better against two-body abrasive wear when compared to same hardness level single-phase martensitic steels [24]. However, here it seems that softer martensitic structure forms thicker white tribolayer than the harder martensite. The white layer then cracks and peels off due to impact wear. Significantly harder samples prevented the formation of the brittle surface layer and withstood more impacts and grooving.

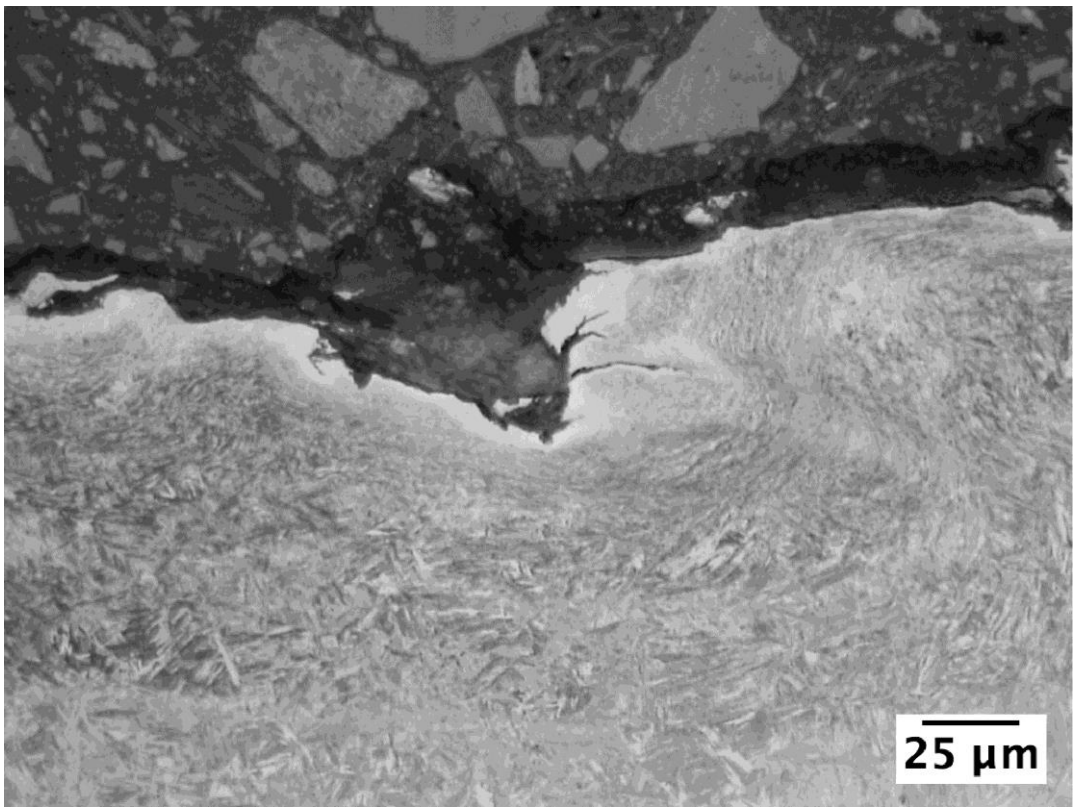

Figure 12: *Optical microscope image of sample 920-250 with embedded granite particle.*

The current tests showed that the highest initial surface hardness provided the best wear performance in laboratory scale impact-abrasion tests. Direct quenching produced high hardness values while interrupted quenching resulted in lower hardness, but better impact toughness. The composition was the same for all tested steel variants, and all variants had martensitic microstructure. The measured amount of retained austenite was low, even for the samples produced with quenching stopped between M_s and M_f temperatures. The outcome of the current paper is that the wear rate is lowest for the hardest martensitic steels, but it was shown that an ultra-high strength steel with well-balanced impact toughness and hardness properties can be produced by novel interrupted quenching method combined with thermomechanically controlled processing.

6. CONCLUSIONS

- High-hardness laboratory rolled steel was tested for wear performance with impeller-tumbler wear testing device. Processing method was thermomechanically controlled processing (TMCP) with different finish rolling temperatures (FRT). Direct quenching (DQ) and interrupted quenching with quenching finish temperature (QFT) of 250 °C were applied. Nearly 700 HV10 surface hardness was achieved with the direct quenched samples. All tested variants had martensitic microstructure.
- Varying the finish rolling temperature (920, 850 and 780 °C) resulted in different prior austenite grain size and shape. Decreasing the FRT produced elongated and more pancaked grain structure. However, the impact toughness was not significantly improved by rolling in the non-recrystallization (NRX) regime.
- The interrupted quenching provided greater impact toughness values. The direct quenched variants showed low toughness even at room temperature. In contrast, the surface hardness was lower for QFT

variants. The best balance of impact toughness and hardness was achieved with 780 °C FRT combined with 250 °C QFT.

- Surface hardness was the main controlling factor of wear in impeller-tumbler tests. The hardest samples exhibited the lowest mass loss. The correlation between surface hardness and wear resistance was almost linear. The high hardness prevented the penetration of abrasives into the surface. Brittle tribolayer was formed on the surface of samples with lower hardness, which seemed to fracture under impact wear. Adiabatic shear bands were discovered on all samples.

ACKNOWLEDGEMENTS

The work has been done within FIMECC Ltd and its already finished *Demanding Applications* (*DEMAPP*) and on-going *Breakthrough Steels and Applications* (*BSA*) programs. We gratefully acknowledge the financial support from Tekes and the participating companies. The corresponding author would also like to express his gratitude for the support provided by the University of Oulu Graduate School through Advanced Materials Doctoral Program (ADMA-DP).

REFERENCES

1. C. Ouchi. Development of Steel Plates by Intesive Use of TMCP and Direct Quenching Processes. ISIJ International 41(6) (2001), pp. 542-553.
2. A.J. Kaijalainen, P.P. Suikkanen, T.J. Limnell, L.P. Karjalainen, J.I. Kömi, D.A. Porter. Effect of austenite grain structure on the strength and toughness of direct-quenched martensite. Journal of Alloys and Compounds 577S (2013), pp. 642-648.
3. A.J. Kaijalainen, P.P. Suikkanen, L.P. Karjalainen, J.J. Jonas. Effect of Austenite Pancaking on the Microstructure, Texture and Bendability of an Ultrahigh-Strength Strip Steel. Metallurgical and Materials Transactions A 45A (2014), pp. 1273-1283.
4. E. Kinnunen, I. Miettunen, M.C. Somani, D.A. Porter, L.P. Karjalainen, I. Alamattila, A. Kemppainen, T. Liimatainen, V. Ratia. Development of a New Direct Quenched Abrasion Resistant Steel. International Journal of Metallurgical Engineering 2(1) (2013), pp. 27-34.
5. G.A. Thomas, J.G. Speer, D.K. Matlock. Quenched and Partitioned Microstructures Produced *via* Gleeble Simulations of Hot-Strip Mill Cooling Practices. Metallurgical and Materials Transactions A 42A (2011), pp. 3652-3659.
6. X. Tan, Y. Xu, X. Yang, Z. Liu, D. Wu. Effect of partitioning procedure on microstructure and mechanical properties of a hot-rolled directly quenched and partitioned steel. Materials Science & Engineering A 594 (2014), pp. 149-160.
7. F. Tariq, A. Baloch. One-Step Quenching and Partitioning Heat Treatment of Medium Carbon Low Alloy Steel. Journal of Materials Engineering and Performance 23(5) (2014), pp. 1726-1739.
8. G. Krauss. Steels: Processing, Structure, and Performance. ASM International, 2005. 613 p.
9. R. Barbosa, F. Boratto, S. Yue, J.J. Jonas. The influence of chemical composition on the recrystallization behaviour of microalloyed steels, in: THERMEC ‘88. Proceedings. Iron and Steel Institute of Japan, Tokyo, 1988, p. 383-390.
10. R.L. Higginson, C.M. Sellars. Worked examples in quantitative metallography. Maney Publishing, 2003. 128 p.
11. V. Ratia, K. Valtonen, A. Kemppainen, V-T. Kuokkala. High-Stress Abrasion and Impact-Abrasion Testing of Wear Resistant Steels. Tribology Online 8(2) (2013), pp. 152-161.
12. A.J Kaijalainen, P.P Suikkanen, L.P. Karjalainen, J.I. Kömi, A.J DeArdo. Effect of austenite conditioning in the non-recrystallization regime on the microstructures and properties of ultra-high strength bainitic/martensitic strip steel, in: 2nd International Conference on Super-high Strength Steels, Verona, 2010. 19 p.
13. X. Deng, Z. Wang, Y. Han, H. Zhao, G. Wang. Microstructure and Abrasive Wear Behavior of Medium Carbon Low Alloy Martensitic Abrasion Resistant Steel. Journal of Iron and Steel Research International 21 (1) (2014), pp. 98-103.
14. I. Kosazu, C. Ouchi, T. Sampei, T. Okita. Hot Rolling as a High-Temperature Thermo-Mechanical Process. In: Proc. Int. symp.. Microalloying ’75, Union Carbide Corporation, New York, USA 1975, pp. 100-114.
15. L. Bracke, W. Xu, T. Waterschoot. Effect of finish rolling temperature on direct quenched low alloy martensite properties. Materials Today: Proceedings 2s (2015), pp. S659-S662.

16. J. Speer, D.K. Matlock, B.C. De Cooman, J.G. Schroth. Carbon partitioning into austenite after martensite transformation. Acta Materialia 51 (2003), pp. 2611-2622
17. D.V. Edmonds, K. He, F.C. Rizzo, B.C. De Cooman, D.K. Matlock, J.G. Speer. Quenching and partitioning martensite – A novel steel heat treatment. Materials Science and Engineering: A 438-440 (2006), pp. 25-34.
18. J.I. Kim, C.K. Syn, J.W. Morris. Microstructural sources of toughness in QLT-Treated 5.5Ni cryogenic steel. Metallurgical Transactions A 14(1) (1983), pp. 93-103.
19. P.P. Suikkanen, A-J. Ristola, A.M. Hirvi, P. Sahu, M.C. Somani, D.A. Porter, L.P. Karjalainen. Effects of Carbon Content and Cooling Path on the Microstructure and Properties of TRIP-aided Ultra-High Strength Steels. ISIJ International 53 (2) (2013), pp. 337-346.
20. J.F Knott. Quantifying the quality of steel. Ironmak. Steelmak. 35 (2008), pp. 264–282.
21. J.W. Morris. Metallurgical control of the ductile-brittle transition in high-strength structural steels, in: Proceedings of the 1998 MRS Fall Meeting - The Symposium Advanced Catalytic Materials, Boston, MA, USA, 1998. Materials Research Society Symposium, Proceedings, 539 (1999), pp. 23-27.
22. A. Sundström, J. Rendon, M. Olsson. Wear behaviour of some low alloyed steels under combined impact/abrasion contact conditions. Wear 250 (2001), pp. 744-754.
23. J. Rendon, M. Olsson. Abrasive wear resistance of some commercial abrasion resistant steels evaluated by laboratory test methods. Wear 367 (2009), pp. 2055-2061.
24. B. Narayanaswamy, P. Hodgson, H. Beladi. Comparisons of the two-body abrasive wear behaviour of four different ferrous microstructures with similar hardness levels. Wear 350-351 (2016), pp. 155-165.
25. B. Dodd, Y. Bai. Adiabatic Shear Localization. Elsevier, 2012. 468 p.
26. V. Ratia, I. Miettunen, V-T. Kuokkala. Surface deformation of steels in impact-abrasion: The effect of sample angle and test duration. Wear 301 (2013), pp. 94-101.
27. N. Ojala, K. Valtonen, V. Heino, M. Kallio, J. Aaltonen, P. Siitonen, V-T. Kuokkala. Effects of composition and microstructure on the abrasive wear performance of quenched wear resistant steels. Wear 317 (2014), pp. 225-232.